

Two-dimensional electron crystals in single and double layers

A.V. FILINOV^{1,2}, M. BONITZ¹, AND YU.E. LOZOVIK²

¹Fachbereich Physik, Universität Rostock Universitätsplatz 3, D-18051 Rostock, Germany

²Institute of Spectroscopy, 142090 Troitsk, Moscow Region, Russia
e-mail: alex@ravel.mpg.uni-rostock.de

Abstract

We present results of Monte-Carlo simulations for finite 2D single and bilayer systems. Strong Coulomb correlations lead to arrangement of particles in configurations resembling a crystal lattice. For binary layers, there exists a particularly rich variety of lattice symmetries which depend on the interlayer separation d . We demonstrate that in these mesoscopic lattices there exist two fundamental types of ordering: radial and orientational. The dependence of the melting temperature on d is analyzed, and a stabilization of the crystal compared to a single layer is found.

Introduction. The properties of a finite number of charged particles ($N \sim 10$) in a single “two-dimensional” layer have been the subject of intensive theoretical and experimental investigation in the last decade [1]-[5]. In particular, if at low temperature the density parameter r_s is increased, transitions from a Fermi liquid to a so-called Wigner molecule [4] and, further, to a Wigner crystal have been found [5]. The interplay between the long-range Coulomb interaction and a shallow confinement potential plays in these systems a prominent role making conventional effective single-particle approximations unreliable. In this connection the predictions of both classical and quantum Monte Carlo methods which treat N-body correlations rigorously, are of great importance, in particular for the theoretical understanding of the solid-liquid crossover. Recently, a new 2D system has attracted the attention of several groups, namely, bilayer structures. The phase diagram of bilayer systems is far more rich compared to single layers. In particular, the formation of Wigner lattices in electronic or ionic bilayers has been predicted, both by classical [6] and quantum-mechanical [7] studies and revealed the existence of distinct structural phases: rectangular, square, rhombic and triangular staggered lattices. The transition between these phases takes place at specific values of the interlayer distance d , when one of the phases becomes energetically favorable and may proceed in continuous or discontinuous manner. However, these predictions have been made for *macroscopic* systems. Here, we extend the analysis of bilayer structures to finite-size systems (e.g. electrons or ions in quantum dots and radio frequency traps, respectively). Our previous investigation of finite single layer structures [5] has revealed that these mesoscopic systems have a richer phase diagram than their macroscopic counterpart, and that the phase diagram strongly depends on the particle number. In this paper, we demonstrate that different crystalline structures are stable in different ranges of the interlayer distance. Moreover, we find that melting may proceed in several stages, and the crystal may be stabilized by choosing a proper value of d .

Model and characteristic parameters. We consider a system of N charged particles of the same type interacting via the repulsive Coulomb potential located in two 2D

layers which are a distance d apart. In each layer a circular symmetric parabolic potential of strength ω_0 is applied. The system is described by the hamiltonian

$$\hat{H} = \sum_{i=1}^N \frac{\hbar^2 \nabla_i^2}{2m_i^*} + \sum_{i=1}^N \frac{m_i^* \omega_0^2 r_i^2}{2} + \sum_{l=1}^2 \sum_{i < j}^{N_l} \frac{e^2}{\epsilon_b |\mathbf{r}_{ij}|} + \frac{1}{2} \sum_{i=1}^{N_1} \sum_{j=1}^{N_2} \frac{e^2}{\epsilon_b \sqrt{\mathbf{r}_{ij}^2 + d^2}}, \quad (1)$$

where $\mathbf{r}_{ij} \equiv \mathbf{r}_i - \mathbf{r}_j$, m^* and ϵ_b are the effective electron mass and background dielectric constant, respectively. We use the following length and energy scales: r_0 , given by $e^2/\epsilon_b r_0 = m^* \omega_0^2 r_0^2/2$, and E_c - the average Coulomb energy, $E_c = e^2/\epsilon_b r_0$. After the scaling transformations $\{r \rightarrow r/r_0, E \rightarrow E/E_c, d \rightarrow d/r_0\}$ the hamiltonian becomes

$$\hat{H} = \frac{n^2}{2} \sum_{i=1}^N \nabla_i^2 + \sum_{i=1}^N r_i^2 + \sum_{l=1}^2 \sum_{i < j}^{N_l} \frac{1}{|\mathbf{r}_{ij}|} + \frac{1}{2} \sum_{i=1}^{N_1} \sum_{j=1}^{N_2} \frac{1}{\sqrt{\mathbf{r}_{ij}^2 + d^2}}, \quad (2)$$

where $n \equiv \sqrt{2} l_0^2 / r_0^2 = (a_B^* / r_0)^{1/2}$, a_B^* is the effective Bohr radius, and $l_0^2 = \hbar / (m^* \omega_0)$, is the extension of the ground state wave function of noninteracting trapped electrons. Further, we define, in analogy to macroscopic systems, $r_s \equiv r_0 / a_B^* = 1/n^2$ [5]. Finally, we introduce the dimensionless temperature $T \equiv k_B T / E_c$ which allows us to define the classical coupling parameter as $\Gamma \equiv 1/T$ [2]. To make reliable calculations in the crystal phase, where the Coulomb energy strongly exceeds the kinetic energy, standard methods, such as Hartree-Fock or density functional theory are not applicable. We, therefore, use classical and path integral (PIMC) Monte Carlo simulations in the classical and quantum regions of the phase diagram, respectively.

Phase boundary of the mesoscopic Wigner crystal in a single layer, $d = 0$. Our simulations revealed that the structure of the clusters in the crystal phase strongly depends on the particle number and results from the competition of two ordering tendencies: for large particle numbers, a triangular lattice is energetically favorable. In contrast, for small N , the particles tend to form shells. For intermediate particle numbers, $N > 40$, only the outer electrons form shells, while the inner part goes over to a triangular lattice structure. These configurations are remarkably stable and are visible even outside the crystal phase. To distinguish the solid and liquid phases, we used the standard Lindemann criterion which is based on the analysis of the magnitude of the inter-particle distance fluctuations, see e.g. [2]. Indeed, our simulations show that these fluctuations exhibit jumps (see Fig 3.a below) which allow us to locate the phase boundary of the crystal. When leaving the crystal, the relative distance fluctuations increase several times which results from particles exchanging their lattice sites or undergoing inter-shell transitions. Interestingly, we find two distinguished crystal phases: first, a completely ordered state and second, a partially (only radially) ordered phase where shells can rotate with respect to each other. The transition between the two phases will be called orientational melting (“OM”), whereas the transition from the radially ordered state to the liquid-like state is radial melting (“RM”). We underline that this phase still resembles the crystal (it still exhibits shell structure). Nevertheless, it is characterized by essentially increased inter-shell exchanges of particles and, therefore, this “Wigner molecule” phase [4] may not be identified with a crystal.

The results for the phase boundaries in the density-temperature plane are summarized in Fig. 1 for various particle numbers. Consider first the line of radial melting “RM”. At low densities, $n < 0.03$, we are in the classical regime, and the phase boundary

is given by critical values of the coupling parameter Γ which, in Fig. 1 corresponds to straight lines from the origin. We found that Γ deviates from the 2D bulk value, $\Gamma_\infty = 137$, e.g. [2], and strongly depends on the cluster size. Further increase of Γ , (reduction of the slope of the straight line), eventually leads to the second phase boundary, labelled “OM” which corresponds to freezing of the inter-shell rotation. At sufficiently low temperature, the electron behavior in this phase is dominated by quantum effects. This becomes particularly clear if the density parameter n is increased. In this case, we observe increasing quantum (zero-point) fluctuations. When the line “OM” is reached, again a jump of the relative distance fluctuations is observed which corresponds to “cold” orientational melting [5]. Finally, increasing n further, leads to the line “RM”, i.e. to cold radial melting of the crystal. From the figure it is clear that each of the two crystal phases exists up to a maximum temperature. This temperature is comparatively low. Using typical parameters of 2D GaAs semiconductors, the maximum temperature of the radially ordered phase is in the range of $1 \dots 5K$.

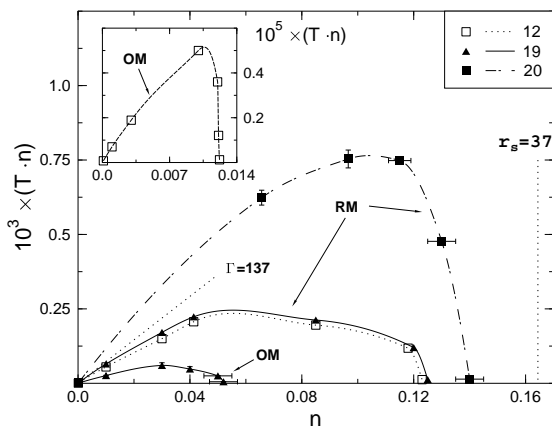


Fig. 1: Phase diagram of the mesoscopic 2D Wigner crystal. “OM” (“RM”) denotes the orientational (radial) melting curves for $N = 12, 19, 20$. Insert shows an enlarged picture of the low-density region. Dotted straight lines indicate the radial melting transition of a macroscopic classical and quantum WC. Brueckner parameter follows from the density by $r_s = 1/n^2$. Shown error bars are typical for all curves.

are arranged into two parallel layers each containing an equal number of particles. For zero separation, $d = 0$, we have just one 2D “atom”. For example, for $2N = 38$, this is a cluster with one electron in the trap center and three shells containing 7, 13 and 17 electrons, respectively. In the opposite limit, $d \rightarrow \infty$, the system consists of two independent clusters with $N = 19$ particles and shell configuration $\{1, 6, 12\}$. Below we provide a detailed investigation of the structural changes between these two limits for the case $N = 19$.

Different crystalline structures can be identified from snapshots of instantaneous configurations (see insets in Fig. 2). In Fig. 3.c we also show particle configurations in both layers projected onto the same plane. To characterize the structural symmetry

Interestingly, the phase boundary of the crystal significantly varies with the number of particles. This dependence is particularly strong for the orientational melting transition, and we find that crystals in so-called magic clusters have unusually high stability. The reason is that these clusters have the highest angular symmetry (the particle numbers on the shells have a common divisor). This is a peculiarity of mesoscopic systems; the strong number dependence of the melting properties vanishes in the limit of a macroscopic system where also the two crystal phases merge into one.

Bilayers, $d \neq 0$. Let us now turn to electron crystallization in two parallel 2D layers. We study a classical bilayer crystal using standard MC simulations. The particles

in each layer we use a suitable order parameter given by

$$G_m(R) = \left\langle \frac{1}{N_l} \sum_j^{N_l} |\phi_m(j)| \right\rangle, \quad \phi_m(j) = \frac{1}{N_j^{nb}(R)} \sum_k^{N_j^{nb}(R)} \exp^{-im\theta_{jk}} \quad (3)$$

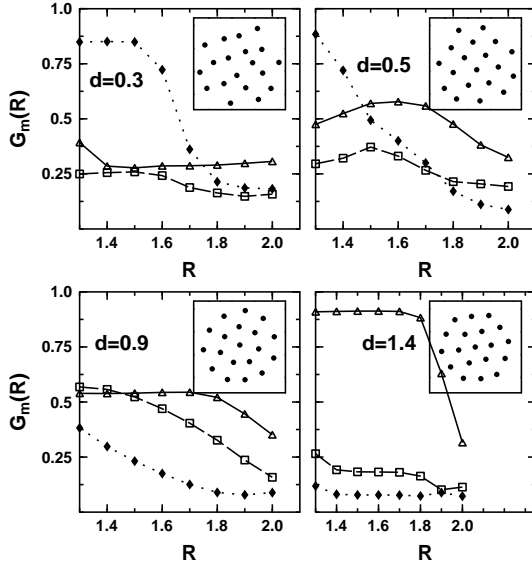


Fig. 2: Order parameter $G_m(R)$, Eq. (3), characterizing the angular lattice symmetry for several values of d . Symbols denote $m = 4$ (diamonds), $m = 5$ (squares) and $m = 6$ (triangles). Insets show the corresponding particle configuration in one layer.

titative criterion for these phase transitions (see Fig. 3.a,b). We define the interlayer ($l \neq m$, $C = N_l N_m$) and intralayer [$l = m$ and $i \neq j$, $C = N_l(N_l - 1)$] distance fluctuations, u^{lm} , and the radial fluctuations with respect to the trap center, u^l , as

$$u^{lm} \equiv \frac{1}{C} \sum_i^{N_l} \sum_j^{N_m} \sqrt{\frac{\langle r_{ij}^2 \rangle}{\langle r_{ij} \rangle^2} - 1} \quad \text{and} \quad u^l \equiv \frac{1}{N_l} \sum_i^{N_l} \sqrt{\frac{\langle r_i^2 \rangle}{\langle r_i \rangle^2} - 1}, \quad (4)$$

where N_l and N_m are the number of particles in layer l and m , respectively; r_{ij} is the projection of the distance between particles i and j onto one of the layers; and $\langle \dots \rangle$ denotes an ensemble average.

First, we start to decrease the interlayer distance from the limit $d \rightarrow \infty$. The configuration $\{1, 6, 12\}$ corresponding to two independent clusters does not change up to $d \approx 0.9$. The temperature dependence of the inter(intra)-layer pair distance fluctuations $u^{lm}(u^l)$, Eq. (4), for $d = 1.4$ are shown in Fig. 3.a. The two jumps in the behavior of the fluctuations correspond to the two melting transitions. First, orientational melting takes place in both layers simultaneously. That means that the shells with 6 and 12 particles are orientationally disordered and can rotate relative to each other, as in the single-layer system. This melting takes place at a temperature $T_o \approx 2.5 \cdot 10^{-3}$. Notice that the intra and interlayer fluctuations differ significantly

where the first sum is taken over the N_l particles in the inner part of the crystal (all particles except those on the outer shell), and the sum over k runs over all intralayer neighbors of particle j within a circle of radius R . $m = 2, 3 \dots$; and θ_{jk} is the angle between some fixed axis and the vector connecting the j -th particle and its k -th neighbor. For a triangular lattice, the order parameter G_6 approaches one, whereas for a square(rhombic) lattice, G_4 becomes close to unity. We also consider the magnitude of the relative intra/inter-layer distance fluctuations. In the vicinity of orientational and radial melting, the fluctuations, Eq. (4), show a strong increase, thus providing a suitable quan-

which shows that interlayer correlations are comparatively small which allows the shells in the two layers to rotate independently of each other (Fig. 3.a, upper part). Radial melting sets in at a higher temperature, $T_r \approx 6.5 \cdot 10^{-3}$, which is the same temperature as was found for single-layer systems [5].

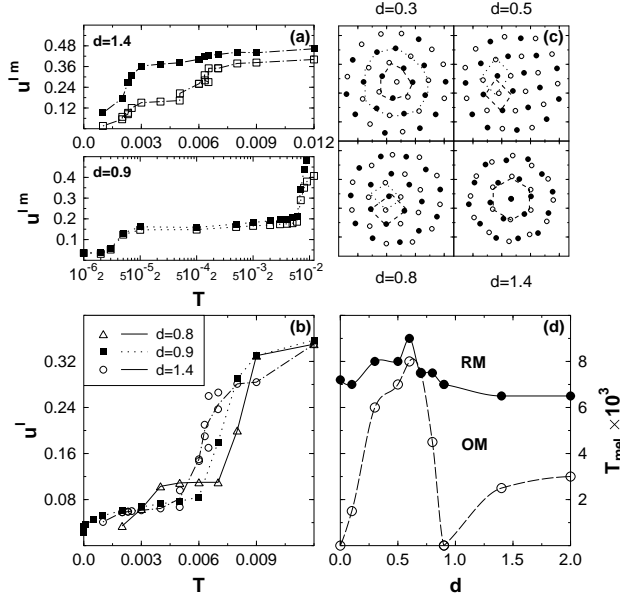


Fig. 3: Crystallization in a classical bilayer system for varying interlayer distance d . Left three figures: Relative two-particle distance fluctuations u^{lm} for particles from the same layer (open symbols) and from different layers (full symbols) and radial fluctuations u^l , Eq. (4). Upper right figure shows snapshots of the crystal structure for $T = 3 \cdot 10^{-3}$. Full and open symbols denote particles from different layers, thin lines are guide for the eye to underline the cluster symmetry. Lower right figure shows the critical temperature of the radial (RM) and orientational (OM) melting transitions versus d .

system. The critical temperature of this transition is significantly lower, $T_o \approx 5 \cdot 10^{-6}$, which is a result of the modified shell configuration. Total melting occurs at $T_r \approx 7 \cdot 10^{-3}$.

Now we consider the distance $d = 0.8$. The interlayer correlations lead to the formation of staggered rhombic lattices in the inner parts of the clusters. The interesting point here is that these staggered lattices still have the possibility to rotate relative to the outer shells. This takes place at $T_o \approx 4.5 \cdot 10^{-3}$. This essential increase of the orientational melting temperature (compared to the case $d = 0.9$) is due to the fact that the outer and inner shells begin to lose angular symmetry (which is similar to $d = 0.5$, see inset of Fig. 2). Close inspection of this figure shows that some particles (in the top part) are moved inbetween the shells which effectively hampers rotation of the shells. The calculated radial distribution functions (not shown) also confirm this conclusion. In addition to the peaks corresponding to the two shells (for $d \geq 0.9$), here a third maximum arises inbetween. Radial melting sets in at $T_r \approx 7.5 \cdot 10^{-3}$, which is an important increase of the stability against radial disordering compared to larger values of d , cf. Fig. 3.b.

Decreasing the interlayer distance to $d = 0.9$ leads to redistribution of particles on the shells. The cluster configuration $\{1, 7, 11\}$ in each layer becomes energetically favorable, cf. Fig. 2. These changes in the cluster symmetry lead to quite different temperatures of orientational melting. Now the inner shells in the two layers are “frozen” and cannot rotate with respect to each other. However, they can rotate together relative to the (frozen) two outer shells which is clearly seen in the coinciding inter and intralayer distance fluctuations, Fig. 3.a, lower part. This is a new type of disordering transition which is missing in the single-layer

At interparticle distances in the range $d = 0.5 \dots 0.7$ the angular shell symmetry in the system is practically lost and the particle configuration in each layer resembles a rhombic lattice, cf. Fig. 3.c. This leads to drastic changes in the behavior of the fluctuations: orientational and radial transitions take place approximately at the same temperature, $T_o \approx 7 \dots 8 \cdot 10^{-3}$ and $T_r \approx 7.5 \dots 9 \cdot 10^{-3}$, cf. Fig. 3.d. Further decrease of the interlayer separation up to $d = 0.3$ gives rise to another symmetry change, to formation of a rectangular lattice in each layer, cf. Fig. 2. Interestingly however, the system as a whole regains spherical symmetry: as is clearly seen in Fig. 3.c, all particles together arrange into a spherically symmetric cluster of $2N = 38$ particles with the shell configuration $\{1, 7, 13, 17\}$. This restoration of spherical symmetry causes the temperature of the orientational melting to drop significantly around $d = 0.3$, cf. Fig. 3.d. The obvious conclusion is that the interlayer correlations already dominate the behavior of the clusters, and the system has become effectively a single-layer structure. When $d \rightarrow 0$, we again observe all properties of a single-layer crystal, including the critical values of temperatures for radial and orientational melting, $T_o \approx 1 \cdot 10^{-6}$ and $T_r \approx 7.2 \cdot 10^{-3}$, respectively.

In summary, we have presented a detailed analysis of Wigner crystallization of finite electron systems in one and two layers. In particular, we discussed the influence of interlayer correlations on the crystal phase. We have shown that, when d is reduced, the clusters first lose spherical symmetry and transform into a rectangular (rhombic) lattice. Finally, at low d , a spherical arrangement is re-established when all particles effectively form a single layer. We have found that this intermediate range of d -values provides an additional stabilization of the Wigner crystal, and the melting temperature may rise by up to 50% (confirming the previous finding for macroscopic systems [6]). The same tendency is expected to hold in mesoscopic clusters in the quantum range (very low temperature): interlayer correlations should significantly reduce the critical value of r_s [5] up to $r_s \rightarrow 2/3r_s$ which should improve prospects for an experimental observation of electron(hole) crystallization in semiconductor heterostructures even at zero magnetic field.

Acknowledgements

This work is supported by the Deutsche Forschungsgemeinschaft (Schwerpunkt "Quantenkohärenz in Halbleitern") and the NIC Jülich.

References

- [1] R.C. Ashoori, Nature (London) **379**, 413 (1996); N.B. Zhitenev et al., Phys. Rev. Lett. **79**, 2309 (1997)
- [2] V.M. Bedanov, and F.M. Peeters, Phys. Rev. B **49**, 2667 (1994), and references therein
- [3] Yu.E. Lozovik and E.A. Rakoch, Phys. Rev. B **57**, 1214 (1998); A.I. Belousov and Yu.E. Lozovik, JETP Lett. **68**, 858 (1998)
- [4] R. Egger, W. Häusler, C.H. Mak, and H. Grabert, Phys. Rev. Lett. **82**, 3320 (1999)
- [5] A.V. Filinov, Yu.E. Lozovik and M. Bonitz, phys. stat. sol. (b) **221**, 231 (2000); Phys. Rev. Lett., accepted for publication (2001)
- [6] G. Goldoni and F.M. Peeters, Phys. Rev. B **53**, 4591 (1996); I.V. Schweigert, V.A. Schweigert, and F.M. Peeters, Phys. Rev. Lett. **82**, 5293 (1999)
- [7] F. Rapisarda and G. Senatore, p. 529 of *Strongly Coupled Coulomb Systems*, G. Kalman et al. (eds.), Plenum Press, New York, (1998)